

Elsevier Editorial System(tm) for Palaeogeography, Palaeoclimatology, Palaeoecology
Manuscript Draft

Manuscript Number:

Title: Late Neogene Paleoclimate and Paleoenvironment Reconstructions from Pipe Creek Sinkhole, Indiana, USA

Article Type: Research Paper

Section/Category:

Keywords: Neogene, Pliocene, Karst, Isotope, Lacustrine, Terra rossa

Corresponding Author: Mr. Aaron Jacob Shunk, M.S.

Corresponding Author's Institution: Baylor University

First Author: Aaron Jacob Shunk, M.S.

Order of Authors: Aaron Jacob Shunk, M.S.; Steven G Driese, PhD; James O Farlow, PhD; Michael S Zavada, PhD; Mohammad K Zobaa, M.S.

Manuscript Region of Origin:

Abstract: The Late Neogene represents warm Earth conditions immediately prior to the development of extensive northern hemisphere glaciation, and this period in Earth history may therefore provide the best available analog for the projected outcome of continued global warming. There are few interior continental sites of Late Neogene age from the eastern half of North America and subsequently very little is known about the conditions characterizing climate. The Early Pliocene (~5 Ma) Pipe Creek Sinkhole (PCS) includes the sediment fill of a complex karst environment that developed in north-central Indiana, USA (Lat. 40° 27' 25.4", Long. 85° 47' 37.2"). The site includes more than 3 m of high-chroma, red-colored silty-clay sediment interpreted to be terra rossa. The $\delta^{13}\text{C}$ values PCS terra rossa average $-20 \pm 0.7\text{‰}$ PDB, and are interpreted to represent sediment deposited in a closed cave system under high temperatures and with well-drained soils. An in-situ paleosol at the top of the terra rossa represents a transition from a closed cave to an open environment that eventually flooded, thereby becoming a small pond. $\delta^{13}\text{C}$ values from lacustrine

sediments with organic matter derived dominantly from algae average -20.6‰ and suggest the pond was stagnant and enriched with bicarbonate from the underlying limestones or via aquifers. Pond sediments include abundant vertebrate fossils, which are broadly consistent with those inhabiting an open ecosystem such as a savannah or parkland. However, the PCS pollen includes low taxonomic diversity that is dominated by pine with some hickory and flowering plants, but no grass pollen. It is likely that the pollen assemblage represents a local pine dominated ecosystem associated with the pond paleoenvironment, such as a riparian community, and that the greater landscape was drier and open. An alternative hypothesis is that the climate became wetter and initiated the formation of the pond, and an early succession forest ecosystem developed.

1 **1. Introduction**

2 *1.1 Background*

3 The Pipe Creek Sinkhole (PCS) is located in Grant County, Indiana (Fig. 1) and
4 contains a paleoclimate record that is especially significant because it is Late Miocene or
5 Early Pliocene and represents warm-Earth conditions immediately prior to the
6 development of extensive northern hemisphere glaciation. Understanding paleoclimatic
7 records from this period may provide critical information for predicting the outcome of
8 global warming.

9 Although during the Early Pliocene (5 to 3 Ma) many of the external factors that
10 determine climate, such as intensity of incident sunlight, global geography, and
11 atmospheric concentration of carbon dioxide were similar to those operating today, the
12 climate was nevertheless greatly different with elevated temperatures at polar regions and
13 continental glaciers absent from the northern hemisphere, which made sea-level much
14 higher than today (Federov et al., 2006). One distinct difference between the Early
15 Pliocene and today was the global ocean circulation pattern. At 4.6 Ma a critical step
16 occurred in the gradual closure of the Central American seaway and, as a consequence,
17 the Atlantic Ocean circulation pattern changed significantly to the modern pattern with
18 the development of strong North Atlantic Deep Waters (NADW) and intensification of
19 the Gulf Stream (Haug and Tiedemann, 1998). Furthermore, there is abundant evidence
20 that the equatorial Pacific Ocean lacked the east-west temperature gradient present today
21 and that oceanic sea surface temperatures (SST) resembled those present during El Niño
22 events before 3 Mya (Wara et al., 2005; Ravelo et al., 2006). This is significant because
23 the PCS is located in a region that is currently sensitive to drought during El Niño events,

24 and it appears that late Miocene to early Pliocene paleoclimates resembled the conditions
25 present during modern El Niño events (Molnar and Cane, 2007). There are few other
26 interior continental sites from the eastern half of North America of late Miocene to early
27 Pliocene age, other than the Gray Fossil Site in eastern Tennessee (Shunk et al., 2006),
28 and subsequently very little is known about conditions characterizing the Late Neogene
29 climate of this region. The PCS therefore provides an extraordinary opportunity to
30 evaluate the hypothesis that El Niño-like conditions affected Mio-Pliocene paleoclimate
31 in eastern North America and to compare proxy data with the results of computer models.

32 The primary purpose of this paper is to reconstruct aspects of the
33 paleoenvironment and paleoclimate from PCS sediments and organic matter. In order to
34 do this, we use a combination of field relationships, lithostratigraphy, micromorphology,
35 pollen analysis, and bulk elemental and stable isotope geochemistry.

36 *1.2 Site Description*

37 The Pipe Creek Sinkhole (PCS) includes the sediment fill of a complex karst
38 environment located in north-central Indiana, USA (Fig. 1; Lat. 40° 27' 25.4", Long. 85°
39 47' 37.2"). The PCS developed in dipping limestone flank beds of Silurian reef deposits
40 and contains >5 m of Tertiary sediment overlain by Pleistocene glacial till. The PCS site
41 lies within a 75 m by 50 m (by 11 m deep) sinkhole that probably originated as small
42 cave, the roof of which eventually collapsed, thereby allowing the site to fill with fluvial
43 sediments. During a portion of the depositional history a small pond developed and
44 accumulated sediment containing a diverse fauna and flora (Farlow et al, 2001).

45 The PCS contains a well-preserved sedimentary record comprising multiple
46 depositional facies that include (from oldest to youngest): 1) >3 m of high-chroma, red-

47 colored sediment (Munsell color 2.5YR 3/6 to 10R 3/6) that is dominantly clay, but
48 intercalated with carbonate roof-fall and other bedrock materials varying in size from silt
49 to boulders (Fig. 2a); and 2) a gleyed, dark brown (7.5YR 4/4 to 10YR 3/6) or black-
50 colored (Munsell color 10YR 7/8 to 2.5Y 6/8) facies that includes abundant
51 allochthonous sand, as well as diverse faunal and floral assemblages (Fig. 2b). Hereafter,
52 the underlying red-colored sediment facies and the overlying dark-colored sediment
53 facies are referred to as the *red facies* and *dark facies*, respectively. A light yellow-brown
54 to brown-red paleosol that formed from pedogenic modification of the *red facies* is
55 present in portions of the site. Farlow et al. (2001) analyzed the fauna and flora from the
56 PCS *dark facies* sediment and discovered that plants are represented by a diversity of
57 extant terrestrial and wetland forms, whereas the vertebrate assemblage includes a
58 combination of extant and extinct frogs, turtles, fish, birds, snakes, and small and large
59 mammals, which collectively indicate a Late Hemphillian age for the deposit. Analysis of
60 rodent fossils from the PCS, in association with the other biota, collectively suggests an
61 early Pliocene age of slightly more than 5 Ma for the site (Martin et al., 2002). The fossil
62 bones are rarely articulated or associated, but are generally well-preserved, usually with
63 little surficial or internal weathering. Features of the PCS bones, along with the abundant
64 aquatic plant fossils, suggest that the pond sediments remained saturated during early
65 diagenesis and did not experience fluctuations in water content; this further indicates that
66 the *dark facies* depositional environment was dominantly a permanent pond rather than
67 an ephemeral one (Farlow and Argast, 2006).

68 **2. Methods**

69 *2.1 Field lithostratigraphy*

70 Field lithostratigraphic analysis, sampling, and mapping were conducted as
71 sediment was excavated from the site in various stages. Much of the Tertiary sediment
72 fill of the deposit was disrupted in 1998 when quarrying operations removed the thick
73 layer of glacial till exposing the underlying Late Neogene sediment. Fortunately,
74 relatively intact stratigraphic sections were preserved near very large (4 m diameter)
75 boulders of the local limestone bedrock. In 2003-2005 continued excavations exposed
76 large amounts of sediment, which was photographed and sampled for geochemical and
77 petrographic analysis. Large boulders were removed from the site interior with heavy
78 machinery, thereby exposing additional fresh strata that were available for further
79 analysis. Detailed site maps with surveyed elevations are currently in preparation for
80 publication elsewhere.

81 *2.2 Micromorphology, geochemistry, and palynology*

82 Ten representative samples for thin-section analysis were collected from different
83 stratigraphic levels within the PCS. Samples were dried and then surface-impregnated
84 with resin prior to commercial thin-section preparation. Thirty total bulk sediment
85 samples (with visible fossil wood removed) were collected for $\delta^{13}\text{C}$ and $\delta^{15}\text{N}$, % C, and
86 % N analyses from the PCS sediment. Nineteen samples were collected from the thickest
87 remaining section of the *dark facies* at a 10 cm sampling interval (Fig. 2b), and four
88 samples were collected from various intervals of the paleosol, and three samples were
89 collected at a 1m sampling interval from the top, middle, and bottom of the thickest
90 exposed section of the *red facies*. In addition, more than ten >1cm pieces of well-
91 preserved fossil wood were collected and combined to form a composite sample that
92 represents an “average” isotopic value for fossil tree wood.

93 Powdered bulk samples for geochemical analysis were treated with 10% HCl for
94 2 hours to remove the carbonate fraction. The bulk sediment and wood samples were sent
95 for commercial analysis at the University of Arizona and measured on a Finnigan Delta-
96 plus XL, continuous-flow gas-ratio mass spectrometer coupled to a Costech elemental
97 analyzer. Samples were combusted in the elemental analyzer, and standardization is
98 based on acetanilide for elemental concentration, NBS-22 and USGS-24 standards for δ^{13}
99 C, and the IAEA-N-1 and IAEA-N-2 standards for δ^{15} N. Precision is better than 0.09 for
100 δ^{13} C and 0.2 for δ^{15} N, based on repeated internal standards. Nineteen samples were
101 collected from the PCS *dark facies* for pollen and kerogen analysis and processed in the
102 pollen lab of the Biology Department at East Tennessee State University. Samples for
103 pollen identification were processed using a modified version of Barss and Williams
104 (1973). Samples processed for kerogen used 10-15 grams of each sample which were
105 disaggregated by crushing in a porcelain mortar. To remove the carbonates, concentrated
106 (35 %) HCl was added to the crushed sample and left for about 24 hours to ensure a
107 complete removal of carbonates. Samples were then washed several times with distilled
108 water until being neutral. To remove the silicates, about 100-150 ml of concentrated (45
109 %) HF was added and left for about five days to dissolve all the silicates and were
110 occasionally stirred. After removing the carbonates and silicates the kerogen residues
111 were separated from the inorganic materials by sieving through a 125 μ m brass sieve and
112 collecting the residue in a 10 μ m nylon sieve. No further oxidation or staining were
113 applied to the residues. A few drops of polyvinyl alcohol were added to the residue for
114 dispersion on glass slides and Canada Balsam was used as a permanent mounting

115 medium. Each slide was examined using transmitted light microscopy at X 200, X 500
116 and X 1000 magnification using a Zeiss Axiophot.

117 **3 Results**

118 *3.1 Field stratigraphical and micromorphological analysis*

119 PCS deposits are unlithified and lithostratigraphic relationships are extremely
120 complex because multiple sediment sources and sediment reworking are inherent to
121 primary deposition of clastic sediment in karst environments. The lithostratigraphy is
122 further complicated by post-depositional sediment slumping, reworking, and soft
123 sediment deformation associated with post depositional alteration that occurred during
124 additional Pliocene sedimentation as well as during Pleistocene glaciation. For example,
125 a portion of the *dark facies* sediment is injected into underlying *red facies* sediment due
126 to soft sediment deformation (Fig. 2c). There is clear evidence of sediment mixing and
127 reworking within some regions of the site (Fig. 2d). In portions of the site, strata are
128 interlayered at cm to m scaled layers of various sediment types (Fig. 2e). At the top of
129 the Tertiary sediment section, there is intercalation of different sediment facies with the
130 glacial cover mass. However, in other areas the sediment sections are intact, with correct
131 vertical stratigraphic relationships preserved for characterization in the field (Fig. 2f). No
132 speleothems are present within the PCS sediments, but the site does include calcite
133 crystals with complex growth patterns on some of the large boulders. Abundant, angular
134 carbonate material, ranging in size from sand to boulders, is present throughout the
135 deposits, but in general, sediment without the carbonate-derived particles is non-
136 calcareous and does not react with acid.

137 The *red facies* sediment matrix is comprised dominantly of clastic material (clay)
138 (Fig. 3a, b) intercalated with coarser-grained (sand and pebble to boulder size) carbonate.
139 Portions of the uppermost *red facies* have been pedogenically modified into an immature
140 paleosol (as discussed in subsequent text), and this paleosol and the unaltered lower-
141 portions of the *red facies* will be considered independently, hereafter. The lower portion
142 of the *red facies* (Fig. 2a) does not contain vertebrates, plant fossils, or root trace fossils
143 and includes very little silt- and sand-sized clastic material. Micromorphologic analyses
144 of the *red facies* sediment matrix reveals the texture commonly has a vuggy-cracked
145 microstructure with abundant yellow clay coatings along planar voids. Cracked
146 microstructure portions of the matrix are defined by shrink fractures with FeMn and
147 FeOOH quasi-coatings (Fig. 3a). Along with the fine-grained matrix there are abundant
148 reworked (rounded) sand-size litho-relics of the same composition as the matrix (Fig. 3b),
149 and the sediment includes abundant angular carbonate clasts.

150 The uppermost portion of the *red facies* is yellow (Munsell color 10YR 7/8 to
151 2.5Y 6/8) to brown (7.5YR 4/4 to 10YR 3/6)- colored sediment that includes bifurcating
152 and tapered root trace fossils, abundant illuviated clay, and abundant FeMn nodules,
153 which collectively indicate that the site includes a paleosol (Fig 3f-h). Roots regularly
154 cross-cut and overprint the *red facies* fractures, which indicate the rooting occurred after
155 the fractures and their associated quasi-coatings developed. Birefringent clay is common
156 with geopetal orientations that formed in multiple generations (Fig. 3h). However, aside
157 from the color change, presence of illuviated clay and isolated rooting, the paleosol
158 includes no other advanced pedogenic features such as distinct soil horizons or ped
159 structure. The paleosol is often yellow, and below the paleosol yellow illuviated clay

160 coatings commonly line macropores in portions of the underlying *red facies*. Some of the
161 yellow clay appears to represent the alteration of the *red facies* sediment, as evidenced by
162 some of the sediment partially altered from red to yellow (Fig. 3b) and abundant
163 illuviated yellow clay beneath the paleosol. In other situations the yellow sediment
164 appears to represent primary deposition as evidenced by micro-laminated (mm-scale)
165 sediment that alternates between yellow clay and FeMn stained laminae, and in
166 decimeter-scale interlayering between yellow and red sediment types (Fig. 2e). The
167 abundance of yellow pore-filling sediment decreases with depth in the profile, but yellow
168 infilling exists in all *red facies* sediment observed (to a depth of 3m).

169 A substantial amount of the *dark facies* was removed by quarry operations prior
170 to our analysis. Remaining in situ sediment had a maximum thickness of 1.9 m (Fig. 2b),
171 but typically occurred in thinner (< 0.5m) sheets blanketing most of the site. The *dark*
172 *facies* lies stratigraphically above the *red facies* and its capping paleosol (Fig. 2f). The
173 *dark* includes all known Tertiary plant and animal fossils discovered from the site. The
174 *dark facies* is similar to the *red facies* because it includes abundant reworked fine sand up
175 to cobble- size litho-relics (Fig. 3c), but the *dark facies* also includes abundant medium-
176 sand-sized quartz grains and quartzite pebbles, which are not present within the
177 underlying *red facies* (Fig. 2b, 3d). The *dark facies* is bedded in places and includes
178 abundant fauna and flora. Fossil wood is generally well-preserved, in some cases
179 retaining visible vascular structure (Fig. 3e), but is commonly impregnated with Fe-Mn
180 giving it a black-color. Micromorphologic analysis reveals that the *black facies* is rich in
181 Fe-Mn nodules (Fig. 3c). Sepic-plasmic clay fabric and isolated FeMn nodules are also
182 abundant within the *dark facies* (Fig. 3c).

183 3.2 Geochemical analysis

184 The $\delta^{13}\text{C}$ values of organic C in bulk sediment samples analyzed from PCS
185 deposits averaged -22.0‰ PDB (± 2.3) (Fig. 4). The *dark facies* sediment averaged 0.9
186 $\%$ (± 0.6) organic carbon (OC), with $\delta^{13}\text{C}$ values averaging -21.9‰ (± 0.6), $\delta^{15}\text{N}$ values
187 averaging 4.5‰ (± 1.0), and C/N ratios averaging 17.5 (± 6.4) (Fig. 4). The *red facies*
188 sediment averaged 0.1 $\%$ OC with $\delta^{13}\text{C}$ values averaging -20‰ (± 0.7) and 0.03 $\%$ N
189 with $\delta^{15}\text{N}$ values averaging 6‰ (± 0.4). The paleosol samples averaged 0.1 $\%$ OC with
190 $\delta^{13}\text{C}$ values averaging -23.7‰ (± 1.1), and 0.1 $\%$ N with $\delta^{15}\text{N}$ values averaging 4.5‰
191 (± 1.0). The composite wood sample contained 47% OC with a $\delta^{13}\text{C}$ value of -25.2‰ ,
192 and 0.7 $\%$ N with $\delta^{15}\text{N}$ value of 5.2‰ (Fig. 5). There is a relationship whereby within
193 the interval from 1.5 to 1.7 m depth in the *dark facies* the C/N values decrease to a
194 minimum, $\delta^{15}\text{N}$ values reach their maximum values, and $\%$ OC is at a minimum value
195 averaging 0.25 (Figs. 4, 5).

196 3.3 Pollen and kerogen analysis

197 PCS pollen and kerogen are generally well-preserved, and palynomorph
198 distribution is dominated by pollen grains of the family Pinaceae (58% of the total count)
199 (Fig. 6a). Freshwater algae and zooclast (derived from freshwater zooplankton) comprise
200 the second highest percentage at about 27%. Pollen of the Juglandaceae is the only other
201 significantly represented woody taxon and comprises about 10% of the flora. There is a
202 notable absence of the common forest and understory tree pollen, and the other recorded
203 taxa (about 5%) include pollen grains of Asteraceae, Polygalaceae and Chenopodiaceae.

204 Samples from depths of 0.9, 0.7 and 0.4 m are generally poor in organic matter.
205 Palynomorphs and amorphous organic matter (AOM) are rare. Opaques and phytoclasts

206 are the dominant kerogen components (Tyson, 1995). Samples from depths of -0.1, -0.2, -
207 0.3, -0.5, -1, -1.1, -1.2 and -1.3 m are rich in organic matter. Palynomorphs and AOM are
208 very rare, whereas opaques and phytoclasts are dominant in these samples. Samples from
209 the -1.4, -1.5, -1.6 and -1.7 m depths are very poor in kerogen content. Palynomorphs and
210 AOM are rare, whereas opaques and phytoclasts are dominant. *Chomotriletes* (fresh
211 water algae) are abundant in samples from -1.6 and -1.7 m depths. *Chomotriletes* are also
212 recorded from the other samples, but are not as abundant as in these two samples. The
213 sample from the -1.9 m depth has especially high organic content. Palynomorphs are
214 common in this sample, whereas AOM are still rare; opaques and phytoclasts are
215 dominant.

216 Pollen of the Pinaceae were investigated using Pearson's (1984) color chart to
217 determine the Thermal Alteration Index (TAI), and the pale yellow to yellow are the
218 dominant exine pointing to a TAI of 1 to 1+, which indicates that the pollen are clearly
219 thermally immature. There is an abundance of equidimensional opaques that are
220 associated with dark brown phytoclasts of total kerogen, which indicates some degree of
221 oxidation in this environment. Overall there is a very high abundance of the small-sized
222 kerogen particles over the large ones (Fig. 6k-l).

223 **4. Interpretations and Discussion**

224 *4.1 PCS paleoenvironment: Red Facies*

225 Figure 7 depicts a summary conceptual model of the geomorphic and stratigraphic
226 development of the PCS. The *red facies* sediment includes no rooting and reduced
227 amounts of yellow clay, and there are no vertebrate fossils present within this sediment.
228 The *red facies* includes abundant angular to sub-rounded limestone clasts that include

229 marine fossils (abundant crinoid stem fossils) and are interpreted to be derived from the
230 local bedrock (Fig. 2a), as well as rounded, coarse sand-sized litho-relicts that are
231 comprised of the same *terra rossa* material, which indicate that the *red facies* includes
232 reworked material (Fig. 3b). The reworked sediment source must have been relatively
233 near the PCS deposit because unlithified clay litho-relicts are easily destroyed when
234 transported great distances. The presence of sand-sized litho-relicts, as well as the coarse-
235 sand-sized carbonate particles within the *red facies*, indicates that there was sufficient
236 energy present to entrain and transport any available coarse clastic material into the basin
237 during the time when the *red facies* was deposited. Thus, the absence of coarse-grained
238 exogenic sediment (such as the abundant quartz clasts present within the *dark facies*), in
239 combination with the lack of vertebrate fossils or root trace fossils in the *red facies*,
240 suggests that this sediment was deposited in a closed karst (cave) environment. The lack
241 of bedding in the *red facies* and persistence of the high-chroma color suggest that the
242 sediment was deposited in a subaerial environment above the water table. Thus, it
243 appears the PCS *red facies* represents deposition within a mostly closed, subaerial
244 depositional environment that received inputs of reworked, fine-grained *terra rossa*
245 sediment that was transferred deeply into the closed karst system, and that the
246 environment was largely closed to the landscape above, which restricted coarse sediment
247 inputs. The large boulders (up to 4 m diameter) are likely remnants of roof and wall fall
248 associated with the breakdown of the karst bedrock.

249 Micromorphological analysis of the PCS *red facies* indicates that the non-
250 carbonate sediment consists of almost exclusively clay-size material (Fig. 3a). The *red*
251 *facies* fabric is dominantly comprised of a cracked microstructure with abundant vugs

252 that are often lined with Fe-oxide stained clay coatings (Fig. 3a), which is remarkably
253 similar to the micromorphology of other described examples of *terra rossa* (Durn, 2003).
254 The cracked microstructure with abundant Fe-Oxide quasi-coatings suggest that the red
255 facies underwent shrink-swell and redoximorphic processes associated with wet/dry
256 cycles. The conspicuous bright red color (between 5YR and 10R) of *terra rossa* is likely
257 a result of the preferential formation of hematite over goethite (i.e. rubification), which
258 occurs under relatively low water activity, high temperature, good aeration (a result of
259 underlying permeable limestone), and/ or high turnover rate for organic matter (Durn,
260 2003). Thick accumulations of *terra rossa* commonly fill karst depressions worldwide,
261 including the region where the PCS occurs (Olson et al., 1980).

262 4.2 Red facies paleoclimate

263 The PCS *red facies* is dominantly comprised of detrital grains that appear to
264 represent *terra rossa* sediment carried into a closed karst (cave) system by water or air
265 currents from the land surface (Fig. 7). Cave sediments generally reflect and record large-
266 scale trends in climate and other geologic or geomorphic variables (Springer, 2005). The
267 Naracoorte cave deposits seem to provide a reasonable analogy for many of the observed
268 features within the PCS. Moriarty et al. (2000) indicate that the Mid-Pleistocene cave
269 fills in the Naracoorte Cave system represent an open, subaerial environment of
270 deposition in which exogenic sediment entered the cave system by both air-fall and water
271 transport from the land surface. This complex depositional setting created debris cones
272 with sedimentary fans at their bases that develop beneath the doline entry points.
273 Interestingly, in this system climate controlled the type of sedimentation deposited,
274 whereby during wet climate phases carbonate and associated speleothems were common

275 and during drier conditions (with a net water deficit) clastic sediment was transported and
276 deposited during episodic storm events, and clastic and chemical depositional events
277 rarely coincided. Thus, the absence of well-developed speleothems or any carbonate
278 cement supports an interpretation that the PCS *red facies* was deposited in relatively dry
279 climatic conditions with a net water deficit. Also, *terra rossa* sediments are common in
280 Mediterranean climates characterized by cool, wet winters alternating with warm, dry
281 summers that create xeric soils (Durn, 2003).

282 The origin of *terra rossa* in Indiana and in general has long been under debate.
283 The view that it represents the residue product from solution of limestone has been
284 rejected by Olsen et al. (1980) because insufficient quantities of insoluble residue in the
285 limestone rock require dissolution of thickness greater than the limestone available, and
286 therefore, *terra rossa* is considered a complex soil with multiple sources of parent
287 material. However, recent field and petrographic evidence presented by Merino and
288 Banerjee (2008) provides evidence that *terra rossa* forms by the replacement of
289 limestone by authigenic clay at a moving metasomatic front with additions of major
290 chemical elements from dissolved eolian dust. Durn (2003) points out that regardless of
291 the source of *terra rossa*, its formation is dependant on the process of rubification in a
292 specific pedoenvironment associated with hard limestone weathering in a Mediterranean
293 climate.

294 The $\delta^{13}\text{C}$ values from cave sediment TOC from Fogelpole Cave and Illinois
295 Caverns in southwestern Illinois demonstrate that paleoclimatic interpretations from cave
296 sediments are typically in good agreement with other proxy records for reconstructing the
297 distribution of C3 and C4 vegetation on the landscape (Panno et al., 2004). The debate

298 about an autochthonous or allochthonous source for terra rossa is significant for
299 understanding PCS *red facies* $\delta^{13}\text{C}$ values. If the *red facies* is a complex soil from the
300 landscape, then the organic material in these sediments likely represents the vegetation on
301 the landscape, and *red facies* $\delta^{13}\text{C}$ values average -20.0 ‰, which suggest a mixture of
302 C3 and C4 plant contributions. However, if the *red facies* represents an in-situ residuum
303 from carbonate dissolution, then its organic material would not represent vegetation
304 growing on the landscape. Unfortunately, after an extensive literature review, we were
305 unable to find other reported $\delta^{13}\text{C}$ values from *terra rossa* for comparison. Thus,
306 paleoclimatic interpretations from the *red facies* $\delta^{13}\text{C}$ values should be made with
307 caution because: 1) it is possible that the $\delta^{13}\text{C}$ values may reflect something besides
308 vegetation in the watershed; and 2) the *terra rossa* sediment TOC is very low (averaging
309 0.1%) and could be modified prior to deposition by microbial processes that can alter the
310 geochemistry of organic matter. $\delta^{15}\text{N}$ values from the *red facies* average 6, but
311 humification typically increases ^{15}N and the N system is generally poorly understood in
312 soils (Kramer et al., 2003) so the data provides little insight about the source of organic
313 material. However, if the *red facies* $\delta^{13}\text{C}$ values are representative of the distribution of
314 C3 and C4 vegetation on the landscape, then a mixed C3 and C4 ecosystem is in good
315 agreement with the Mediterranean-like climates required to form *terra rossa*, the habitat
316 reconstructions from the vertebrate fossils, and the relatively dry conditions necessary for
317 the deposition of clastic cave sediment without carbonate cement or speleothems.

318 *4.3 PCS paleosol and interlayered section paleoenvironment and paleoclimate*

319 The pedogenic alteration of the *red facies* to a paleosol represents a major change
320 in the PCS depositional environments. Because vascular plants require sunlight, the

321 presence of root traces indicates that the cavern had opened prior to pedogenic
322 modification of the *red facies*. The PCS paleosol lacks advanced soil features like distinct
323 soil horizons or a well-developed ped structure, which suggests the paleosol is relatively
324 immature and likely represents a paleoEntisol or paleoInceptisol. Root traces cross-cut
325 Fe-oxide lined voids and cracks in the *red facies*, which indicates that the redoximorphic
326 conditions were present prior to the development of the paleosol.

327 The distinctly yellow color of the uppermost *red facies* and paleosol appears to
328 result from the combination of primary deposition of yellow laminated sediment and/ or
329 the in situ modification of previously deposited *red facies* sediment. The process of
330 yellowing a ferralitic soil likely indicates the transformation of hematite and Al-poor
331 goethite to Al-rich goethite, associated with sediment wetting (Fritsch, et al., 2005). In
332 portions of the site, the top of the *red facies* is inter-layered between red and yellow
333 sediment types (Fig. 2e), which indicates the conditions responsible for deposition of
334 each sediment type alternated through time as sediment was deposited. If yellow
335 sediment represents wetter conditions compared to the red sediment, then the interlaying
336 between sediment types suggests that the PCS paleoenvironment alternated between wet
337 and dry conditions. A possible analogy for the inter-layered sediment within the PCS was
338 described in the Naracoorte Cave (Australia) system by Moriarty et al. (2000).
339 Interestingly, alternating wet- and dry-climate phases controlled the type of
340 sedimentation within the Naracoorte cave deposits and the sedimentation style was inter-
341 layered in a manner similar to that in the PCS. However, it is unclear if the alternation
342 between wet and dry paleoenvironmental conditions relates to an increase of moisture
343 due to the opening to the land surface or to oscillations in paleoclimate.

344 The paleosol $\delta^{13}\text{C}$ values average -23.7 ‰, which are more negative than those of
345 the underlying *red facies* parent material. Because humification during pedogenesis
346 typically increases ^{13}C due to a loss of lighter ^{12}C via microbial respiration (Kramer et al.,
347 2003), the soil $\delta^{13}\text{C}$ values likely reflect additional contributions of organic material
348 derived from C3 plants to the sediment during pedogenesis (e.g., from the addition of
349 root remains) rather than humification.

350 *4.2 Dark facies paleoenvironment*

351 The *dark facies* includes abundant sand-sized and coarser clastic sediment as well
352 as fossil wood and bone derived from the land surface. The *dark facies* sediment onlaps
353 the paleosol (Fig. 2f), which indicates that the *dark facies* was deposited after the site
354 opened to the surface. Thus, at some point following the opening of the PCS environment
355 to the land surface, the PCS flooded and it appears that a ponded environment developed.
356 The development of a pond on top of *red facies* sediment that was deposited above the
357 water-table may relate to the opening of the karst environment to the surface, which may
358 have provided additional water to the environment producing a perched pond.
359 Alternatively, the development of the pond may relate to the development of wetter
360 climatic conditions and an increase to the water-table. A similar increase of the water-
361 table and an associated filling of karst environments with water have been documented in
362 Florida and Georgia due to a climate shift to wetter conditions that occurred at ~8,500 ^{14}C
363 yr BP (Filley et al. 2001). Taphonomic features of the PCS vertebrate fossils, in
364 combination with the presence of abundant aquatic flora and fauna, suggest that the pond
365 environment persisted for an extended interval rather than being repeatedly ephemeral
366 (Farlow and Argast, 2006). However, minor amounts of sepic-plasmic (bright clay)

367 fabrics and in situ Fe-Mn nodules within the *dark facies* (Fig. 3d) indicate that the *dark*
368 *facies* sediments experienced wet and dry periods, but the timing for the establishment of
369 freely drained conditions is unclear.

370 The deepest *dark facies* strata were deposited into a sub-basin cut into the
371 underlying *red facies* sediment and located between two large boulders that created a
372 deepened channel. It is possible the opening of the site to the surface introduced higher
373 energy storm-water flows that scoured into, and eroded away, portions of the previously
374 deposited *red facies* sediment. The *dark facies* includes abundant litho-relics, which
375 indicate the sediment has been reworked, and the angular shape of the grains indicates
376 these sediments are derived from a very nearby source (Fig. 3d). Illuviated clay within
377 some of the reworked litho-relics suggests that the sediment was transported from a
378 subaerially exposed environment such as a soil (i.e., they are pedo-relics), which
379 indicates that portions of the pond sediments were exposed at intermittent periods during
380 the history of the pond.

381 C/N ratios, $\delta^{13}\text{C}$, and $\delta^{15}\text{N}$ values from sediment total organic carbon (TOC)
382 provide a powerful tool for understanding a lacustrine environment and for reconstructing
383 paleoclimate. Meyers (1994) showed that in appropriate lacustrine environments
384 elemental C/N ratios and stable C isotope values appear to retain paleoenvironmental
385 information for multi-Myr periods. This is useful because elemental C/N ratios from
386 TOC preserved in pond sediment can be used to distinguish algae (endogenetic) and land
387 plant sources (dominantly exogenetic) of organic material, because land plants include
388 abundant support tissue that results in land plant C/N ratios > 20 , whereas algae C/N
389 values range between 4 and 10. Carbon isotopic ratios are useful to distinguish between

390 plants using the C3 (Calvin-Benson) and C4 (Hatch-Slack) pathways because C3 plants
391 have $\delta^{13}\text{C}$ values averaging -27 ‰ (PDB) and C4 plant values average -14 ‰ (PDB).
392 Freshwater algae use C3 plants use pathways and typically utilize dissolved CO_2 in the
393 aquifer, which is usually in isotopic equilibrium with atmospheric CO_2 . Therefore, under
394 normal circumstances algal $\delta^{13}\text{C}$ values are the same as land plant values, whereas the
395 source of inorganic C for marine algae is dissolved bicarbonate, which creates organic
396 matter with $\delta^{13}\text{C}$ values between -22 and -20‰ (Meyers, 1994). However, Brenner et al.
397 (1999) indicate that the $\delta^{13}\text{C}$ geochemical system can be complex in some lacustrine
398 settings such as a small, shallow, and potentially stagnant karst environment, as
399 suggested here for the PCS. There are multiple factors that influence the $\delta^{13}\text{C}$ of
400 autochthonous sedimented organic matter including: (1) the rate of atmospheric CO_2
401 exchange, (2) carbonate weathering, (3) the source of C used for primary production, and
402 (4) in-lake rates of photosynthesis. For example, many algae and aquatic vascular plants
403 are capable of utilizing CO_2 from bicarbonate ions when free CO_2 is in very low supply
404 and HCO_3^- is abundant, which generally occurs in stagnant environments or during
405 periods of rapid primary production. Also, during periods of high primary productivity,
406 algae discriminate against ^{13}C and preferentially utilize ^{12}C , which can deplete the light
407 isotope (^{12}C) in the photic zone and produce algae with increased $\delta^{13}\text{C}$ values.
408 Furthermore, some rooted submersed aquatic vegetation have higher $\delta^{13}\text{C}$ values than
409 other C3 plants (-12.8 to 15.9 ‰) because C assimilation is more difficult in water
410 without access to atmospheric CO_2 (Brenner et al. 2006). Under such conditions, it is
411 possible for $\delta^{13}\text{C}$ values of lacustrine algae to resemble typical marine algae values of -
412 22 to -20 ‰. Thus, if the PCS pond was stagnant, maintained high rates of primary

413 productivity, or included abundant submersed aquatic vegetation, then organic matter
414 from autochthonous sources may have included greater $\delta^{13}\text{C}$ values that can resemble a
415 C4 plant influence.

416 The $\delta^{15}\text{N}$ values appear to maintain their primary values in well-preserved
417 lacustrine sediments, and N-isotopes offer a rough estimate for the source of organic
418 material into a lacustrine basin because $\delta^{15}\text{N}$ values of algae average 8 ‰, whereas land
419 plants average 1 ‰ (Meyers and Ishiwatari, 1993). However, it has been shown that
420 some individual autochthonous vegetation types (such as rooted and submersed aquatic
421 vegetation) do not display distinct $\delta^{15}\text{N}$ values, which makes N-isotopes less useful for
422 distinguishing sources of organic material in environments that potentially include these
423 plants (Brenner et al. 2006).

424 The presence of abundant charophyte cysts and fossil wood within the PCS
425 deposits are clear indicators that the PCS received organic matter from both
426 autochthonous and allochthonous sources. C/N values of *dark facies* sediment (from
427 which visible fossil wood was removed) average 17.5 ‰ and generally indicate the
428 sediment TOC includes a mixture of algal and vascular land plant contributions (Fig. 5),
429 which is consistent with the $\delta^{15}\text{N}$ values that average 4.5 (Fig. 4). However, samples
430 between 1.5 and 1.7m depth that maintain C/N values averaging 6.1, $\delta^{15}\text{N}$ values that
431 average 6.4 ‰, and therefore, have C/N ratios and $\delta^{15}\text{N}$ values that are consistent with
432 organic matter derived dominantly from algae (Fig. 5). Furthermore, this zone includes
433 abundant *Chomotriletes* (fresh water algae) grains and very low total kerogen. Thus,
434 collectively these proxy data strongly suggest that this depth interval received dominantly
435 algal contributions to the sediment TOC record. Interestingly, the $\delta^{13}\text{C}$ values from

436 these depths average -20.6 ‰, and in figure 5 these samples plot as marine algae, which
437 strongly suggest that PCS autochthonous algae maintained increased $\delta^{13}\text{C}$ values. The
438 low %TOC (averaging 0.25%) from the 1.5 to 1.7 m depth interval suggests that
439 productivity was not great during the deposition of these sediments. Thus, the
440 geochemical data and presence of abundant algal cell counts from these depths are
441 consistent with the presence of algae (and possible other macrophytes) that utilized
442 bicarbonate for photosynthesis (Fig. 5), and this interval provides strong evidence that the
443 PCS pond sediment includes considerable contributions of organic material derived from
444 algae with high $\delta^{13}\text{C}$ values that arose from their use of HCO_3^- for photosynthesis. A
445 similar modern environment is described for Mud Lake (located in Florida, USA), which
446 shifted from a dominant organic matter source of grasses and surrounding emergent
447 vegetation that utilized atmospheric CO_2 to submerged and floating macrophytes as well
448 as phytoplankton using dissolved CO_2 or bicarbonate for photosynthesis (Filley et al.,
449 2001).

450 The remainder of the PCS *dark facies* has higher C/N ratios, lower $\delta^{15}\text{N}$ values,
451 and abundant kerogen relative to the 1.5 to 1.7 m depth interval, which indicates that
452 TOC likely represents a mixture of vascular land plant and algal contributions. The $\delta^{13}\text{C}$
453 values from the remainder of the deposits average -22 ‰, and are consistent with
454 dominantly algae mixed with small amounts of organic material derived from C3
455 vascular plants characterized by relatively high $\delta^{13}\text{C}$ values (averaging -25.2 ‰) and
456 C/N ratios (averaging 67.6). Additionally, the apparent shift from sediments with organic
457 matter derived dominantly from algae between depths of 1.5 to 1.7 m to a mixed source of
458 algae and vascular wood organic material up-section suggests that the *dark facies*

459 stratigraphy is not mixed or time averaged and therefore represents a time series. This
460 observation is further supported by the presence of cm-scale laminations within the same
461 portion of the *dark facies*.

462 4.4 PCS *dark facies* paleoclimate

463 The PCS *dark facies* includes a well-preserved vertebrate fauna and a flora that
464 includes abundant fossil wood and pollen, which provide multiple proxies for
465 paleoclimate reconstruction. Farlow et al. (2001) indicated that the vertebrate fossil
466 assemblage and floral assemblage includes a mixture of aquatic and terrestrial forms that
467 likely represent a mixture of the local inhabitants of the PCS pond as well as plants and
468 animal derived from an open savannah-like ecosystem with trees nearby. The composite
469 sample of fossil wood indicates that the vascular C3 wood had an average $\delta^{13}\text{C}$ value of
470 -25.2‰ . Cerling et al. (1997) indicated that terrestrial C3 land plants can have a
471 considerable range of $\delta^{13}\text{C}$ values because in water-stressed ecosystems plants are
472 enriched in ^{13}C and can maintain $\delta^{13}\text{C}$ values as high as -22‰ , whereas in forest
473 ecosystems with closed canopies plants can have values as low as -35‰ due to the
474 recycling and depletion of ^{13}C in the air beneath the tree canopy. Also, potential
475 differences in the carbon isotopic composition of the atmosphere influence terrestrial
476 plant $\delta^{13}\text{C}$ values as variations in the isotopic composition of atmospheric CO_2 mirror
477 changes in global C-cycling (Arens et al. 2000). Thus, a value of -25.2‰ for C3 plant
478 fossil wood suggests that the trees likely grew under slightly water-stressed conditions or
479 that the carbon isotopic composition of the atmosphere was slightly heavier during the
480 Early Pliocene (Fig. 5).

481 Pollen counts from the PCS *dark facies* indicates that pollen from the family
482 Pinaceae (Pine) (58%) represent the major palynomorph element followed by algal
483 remains and zooclasts (27%). The only other dominate woody species is Juglandaceae
484 (Hickory) (10%). Pollen from an array of associated forest trees and understory plants are
485 absent from the PCS and would be expected if this represented a closed canopy forest.
486 The occurrence of pollen of the Asteraceae (Daisy), and Chenopodiaceae (Goosefoot)
487 (5%) (Fig. 6) suggest a disturbed habitat. The occurrence of the Polygalaceae (Milkwort)
488 is often associated with wetland habitats and reinforces the occurrence of permanent
489 standing water. This coupled with the abundance of algal remains, and zooclasts further
490 supports the presence of a small, stagnant pond that formed in collapsed karst
491 environment with limited clastic input. The pollen assemblage is low in taxonomic
492 diversity, and probably represents input from a very local environment. The presence of a
493 pine – hickory woodland or savanna (compared to a stratified forest) suggests that
494 disturbance was important part of the local ecosystem (Platt, 1999 and references
495 therein). Thermal Alteration Index (TAI) of the pollen of the Pinaceae indicate that the
496 organic matter is thermally immature. The occurrence of charred phytoclast and
497 amorphous organic material are probably a result of oxidation by fire. This coupled with
498 the abundance of large herbivores may have maintained this habitat as a Pine-Hickory
499 woodland / savanna with an understory of Asteraceae and Chenopodiaceae, both
500 indicative of disturbed habitats.

501 The $\delta^{13}\text{C}$ values from the pond sediments average -22 ‰ (PDB), with C/N values
502 averaging 17.5, and under normal circumstances these values would suggest that the
503 organic matter is composed of a mixture of algae and terrestrially derived vascular land

504 plants and includes a significant contribution of C4 grasses (Fig. 5). However as
505 discussed previously, it appears that the organic material in PCS has less negative $\delta^{13}\text{C}$
506 values possibly derived from the algae or freshwater zooplankton that utilized abundant
507 bicarbonate as a carbon source. Thus, the $\delta^{13}\text{C}$ values from the *dark facies* do not
508 provide evidence for C4 grasses, which is consistent with the absence of grass pollen
509 throughout the stratigraphy.

510 **5. Conclusions**

511 The simplest hypothesis for a conceptual model of the geomorphic and
512 stratigraphic development of the PCS is presented in Figure 7. It is consistent with the
513 following basic information: 1) there is an abrupt facies shift from the non-fossiliferous,
514 finer-grained, high-chroma *red facies* sediment to the fossiliferous, gleyed *dark facies*
515 sediment that includes abundant sand; 2) there was development of a paleosol from
516 underlying *red facies* sediment prior to, or concurrent with, the deposition of *dark facies*
517 sediment; and 3) eventually a pond developed and sediment derived from the land surface
518 was subsequently deposited in an open, sub-aqueous environment. Within the PCS there
519 are abundant reworked litho-relics and interlayered sediment layers, which are consistent
520 with sediment that was reworked from a nearby source such as a debris cone. The pond
521 was likely stagnant with algae utilizing bicarbonate for photosynthesis, which is
522 consistent with a small body of water situated in a karst depression in such a way that
523 mixing of atmospheric CO_2 and water was restricted.

524 The PCS includes a >3 m succession of *terra rossa* with $\delta^{13}\text{C}$ values that average
525 $-20 \pm 0.7\%$ PDB, and PCS clastic cave deposits lack carbonate cement, which also
526 suggest the environment was dry with a net water deficit. *Terra rossa* typically forms in

527 well-drained soils with high temperatures (Mediterranean-like) that produce xeric soils
528 (Durn, 2003). PCS vertebrate fossils are consistent with a mixture of local pond
529 inhabitants and animals from an open savannah-like ecosystem but with trees nearby
530 (Farlow et al., 2001). The mean $\delta^{13}\text{C}$ value of PCS tree fossil wood is -25.2‰ PDB,
531 which suggests that trees did not grow in a closed canopy. Charcoal within the *dark*
532 *facies* suggests that fire was a disturbance factor in this ecosystem. Pollen records from
533 the PCS are dominated by pollen from pine (primarily an early succession plant in the
534 deciduous forest) with contributions from hickory and plants that are indicative of
535 disturbed habitats (Asteraceae and Chenopodiaceae). The pollen record includes low
536 taxonomic diversity and may represent a woodland / savanna habit proximal to the PCS
537 pond itself.

538 An alternative hypothesis to explain the PCS stratigraphy is that the climate
539 became wetter, which initiated the development of the pond itself due to an increase to
540 the water-table. The presence of interlayering sediment types that suggest alternating wet
541 and dry paleoenvironmental conditions are consistent with alternating wet and dry
542 climate conditions prior to the facies shift. If the climate went from relatively dry (*red*
543 *facies*) to wetter conditions (*dark facies*), then this transition may have promoted the
544 development of an early succession pine-dominated forest.

545

546 **Acknowledgments**

547 This research was supported by NSF grant EAR-0207182 and American Association of
548 Petroleum Geologists Foundation: R.E. McAdams Memorial Grant, 2007.

549

550 **References Cited**

- 551 Arens N.C., Jahren, H., Amundson, R., 2000. Can C3 plants faithfully record the carbon
552 isotopic composition of atmospheric carbon dioxide? *Paleobiology*, 26, 137-164.
- 553 Barss, M.S. and G.L. Williams.,1973. Palynology and nannofossil processing techniques.
554 Geological Survey of Canada, 73-26, 26 pgs.
- 555 Brenner, M., Whitmore, T.J., Curtis, J.H., Hodell, Schelske, C.L., 1999. Stable isotope
556 ($\delta^{13}\text{C}$ and $\delta^{15}\text{N}$) signatures of sedimented organic matter as indicators of historic
557 lake trophic state. *Journal of Paleolimnology* 22, 205-221.
- 558 Brenner, M., Hodell, D.A., Leyden, B.W., Curtis, J.H., Kenney, W.F., Gu, B., Newman,
559 J.M., 2006. Mechanisms for organic matter and phosphorus burial in sediments of a
560 shallow, subtropical, macrophyte-dominated lake. *Journal of Paleolimnology* 35,
561 129-148.
- 562 Cerling, T.E., Harris, J.M., MacFadden, B.J., Leakey, M.G., Quade, J., Elsenmann, V.,
563 Ehleringer, J.R., 1997. Global vegetation change through the Miocene/Pliocene
564 boundary. *Nature* 389, 153-158.
- 565 Durn, G., 2003. *Terra rossa* in the Mediterranean region: parent materials, composition
566 and origin. *Geologia Croatica*, 56, 83-100.
- 567 Fedorov, A.V., Dekens, P.S., McCarthy, M. Ravelo, A.C., deMenocal, P.B., Barreiro, M.,
568 Pacanowski, R.C., Philander, S.G., 2006. The Pliocene Paradox (Mechanisms for a
569 Permanent El Niño): *Science* 312, 1485-1489.
- 570 Farlow, J.O., Sunderman, J.A., Havens, J.J., Swinehart, A.L., Holman, J.A., Richards,
571 R.L., Miller, N.G., Martin, R.A., Hunt, R.M., Storrs, G.W., Curry, B.B., Fluegeman,
572 R.H., Dawson, R.R., Flint, M.T., 2001. The Pipe Creek Sinkhole biota, a diverse Late

573 Neogene continental fossil assemblage from Grant County, Indiana. *American*
574 *Midland Naturalist* 145, 367-378.

575 Farlow, J.O., Argast, A., 2006. Preservation of Fossil Bone from the Pipe Creek Sinkhole
576 (Late Neogene, Grant County, Indiana, U.S.A.). *Journal of Paleontological Society of*
577 *Korea*. 22, 51-75.

578 Filley, T.R., Freeman, K.H., Bianchi, T.S., Baskaran, M., Colarusso, L.A., Hatcher, P.G.,
579 2001. An isotopic biogeochemical assessment of shifts in organic matter input to
580 Holocene sediments from Mud Lake, Florida. *Organic Geochemistry* 32, 1153-1167.

581 Fritsch, E., Morin, G., Bedidi, A., Bonnin, D., Balan, E., Caquineau, S., Calas, G., 2005.
582 Transformation of haematite and Al-poor goethite to Al-rich goethite and associated
583 yellowing in a ferralitic clay soil profile of the middle Amazon Basin (Manaus,
584 Brazil). *European Journal of Soil Science* 56, 575-588.

585 Haug, G.H., Tiedemann, R., 1988. Effect of the formation of the Isthmus of Panama on
586 Atlantic Ocean thermohaline circulation. *Nature* 393, 673-676.

587 Kramer, M.G., Sollins, P., Sletten, R.S., Swart, P.K. 2003. N isotope fractionation and
588 measures of organic matter alteration during decomposition. *Ecology* 84, 2021-2025.

589 Martin, R.A., Goodwin, H.T., Farlow, J.O., 2002. Late Neogene (Late Hemphillian)
590 rodents from the Pipe Creek Sinkhole, Grant County, Indiana. *Journal of Vertebrate*
591 *Paleontology* 22, 137-151

592 Merino, E., Banerjee, A., 2008. Terra rossa genesis, implications for karst, and eolian
593 dust; a geodynamic thread. *Journal of Geology* 116, 62-75.

594 Meyers, P.A., 1994. Preservation of elemental and isotopic source identification of
595 sedimentary organic matter. *Chemical Geology* 114, 289-302.

596 Meyers, P.A., Ishiwatari, R., 1993. Lacustrine organic geochemistry-an overview of
597 indicators of organic matter sources and diagenesis in lake sediments

598 Molnar P., Cane, M.A., 2007. Early Pliocene (pre-Ice Age) El Niño-like global climate:
599 Which El Niño? *Geosphere* 3, 337-365.

600 Moriarty, K.C., McCulloch, M.T., Wells, R.T., McDowell, M.C., 2000, Mid-Pleistocene
601 cave fills, megafaunal remains and climate change at Maracoorte, South Australia:
602 towards a predictive model using U-Th dating of speleothems: *Palaeogeography,*
603 *Palaeoclimatology, Palaeoecology* 159, 113-143.

604 Olson, C.G., Ruhe, R.V., Mausbach, M.J., 1980. The *terra rossa* limestone contact
605 phenomena in karst, southern Indiana. *Journal of Soil Science of America* 44, 1075-
606 1079.

607 Panno, S.V., Curry, B.B., Wang, H., Hackley, K.C., Liu, C.-L., Lundstrom, C., Zhou, J.
608 2004. Climate change in southern Illinois, USA, based on the age and $\delta^{13}\text{C}$ of organic
609 matter in cave sediments. *Quaternary Research* 61, 301-313.

610 Platt, W.J. 1999. Southeastern Pine Savannas. In: Anderson, R.C., Fralish, J.S. and J. M.
611 Baskin (Eds.), *Savannas, Barrens, and Outcrop plant Communities of North America,*
612 Cambridge University Press. pgs. 23-51.

613 Ravelo, A.C. Dekens, P.S., McCarthy, M., 2006, Evidence for El Niño-like conditions
614 during the Pliocene: *GSA Today* 16, 4-11

615 Shunk, A.J., Driese, S.G., Clark, G.M., 2006. Latest Miocene to earliest Pliocene
616 sedimentation and climate record derived from paleosinkhole fill deposits, Gray
617 Fossil Site, northeastern Tennessee, U.S.A. *Palaeogeography, Palaeoclimatology,*
618 *Palaeoecology* 231, 265-278.

619 Springer, G.S. 2005. Clastic Sediment in Caves. in Encyclopedia of Caves. Edited by
620 Cluver, D.C. and White, W.B. Elsevier Inc., p. 102-108.

621 Tyson, R.V. Sedimentary Organic Matter: Organic facies and palynofacies. Chapman and
622 Hall, 615 pgs.

623 Wara, M.W., Ravelo, A.C., Delaney, M.L., 2005, Permanent El Niño-Like Conditions
624 During the Pliocene Warm Period: Science 309, 758- 761.

625

626 Figure 1. Map showing the location of the Pipe Creek Sinkhole (PCS). The PCS
627 provides a rare opportunity to study the paleoclimate from the Early Pliocene in a region
628 that lacks extensive late Neogene records.

629

630 Figure 2. Field pictures from the PCS. A) A >1 m thick exposure of silty-clay *red facies*.
631 B) The 1.9 m thick succession of dark facies; notice the white pins that represent
632 locations for sampling at a 10 cm sampling interval. C) Example of soft sediment
633 deformation whereby *dark facies* material (inside stippled lines) was injected into the *red*
634 *facies*. D) Example of sediment mixing of PCS *red facies* and *dark facies* material. E)
635 Interlayering of yellow and red sediment present at the uppermost portion of the *red*
636 *facies* associated with the paleosol and apparent opening of the PCS to the land surface.
637 F) Example of intact stratigraphy showing the underlying *red facies*, the rooted, yellow-
638 colored paleosol, and the *dark facies* sediment.

639

640 Figure 3. Examples of PCS micromorphology. Micrographs C and F-H are in cross-
641 polarized light. A) *Red facies* sediment showing the fine-grained, red-colored matrix with
642 a vuggy-cracked microstructure with Fe-Oxide hypocoatings. Note the infilling of a large
643 void with yellow sediment. B) *Red facies* with reworked litho-relicts. Note the partial
644 yellowing of previously deposited *red facies* sediment that is associated with pedogenic
645 alteration of the red sediment color. C) *Dark facies* sediment showing the abundant
646 exogenic sand grains that are not present in the underlying *red facies*. Note the presence
647 of sepic-plasmic clay fabric and in situ FeMn nodules that indicate the sediment
648 underwent wet-dry conditions. D) *Dark facies* sediment reworked litho-relicts. Note the

649 angular litho-relicts comprised of the same material indicating that these clasts are
650 reworked from a nearby source. E) An example of well-preserved PCS fossil wood. F) A
651 portion of the PCS paleosol showing illuviated clay and abundant FeMn staining and
652 nodules. G) Paleosol showing a bifurcating and tapered root trace fossil backfilled with
653 illuviated clay. H) Illuviated clay with geopetal pendant structure that backfills a
654 macropore.

655

656 Figure 4. Geochemical, kerogen, and pollen distributions within PCS sediments. The
657 dashed vertical line represents the average $\delta^{13}\text{C}$ value of PCS fossil wood. Paleosol
658 samples are collected from multiple areas within the PCS; samples a-c are yellow/ red-
659 colored samples and sample d is a brown/ red colored sample. The sample at -1.3 m was
660 processed and analyzed twice yielding $\delta^{13}\text{C}$ values of -14.7 and -15.9 ‰, respectively.
661 The meaning of these values is unclear because sediment from -1.3 m does not include
662 grass pollen.

663

664 Figure 5. Composite figure of organic matter source identification (Meyers 1994,
665 Brenner, 1999) and variations in isotopic composition of TOC considering both growing
666 conditions and the differences between C3 and C4 photosynthetic pathways (Cerling et
667 al. 1998). Note that the samples from 1.5 to 1.7 m depths plot as derived from algae
668 utilizing bicarbonate for photosynthesis.

669

670 Figure 6. Histogram of percent distribution of PCS pollen and algal cells. Note the
671 abundant pine pollen (Pinaceae) but low amounts of deciduous tree pollen (Juglandaceae)

672 and absence of grass pollen. B- Pinaceae; C,D- Freshwater algae ?; E- Juglandaceae; F,G-
673 Asteraceae; H- Polygalaceae; I, J- Chenopodiaceae; K,L- Phytoclast and Opaque
674 samples.

675

676 Figure 7. A conceptual model of the geomorphic and stratigraphic development of the
677 PCS. A) PCS sedimentation likely initiated in closed (cave) subaerial depositional
678 environment that accumulated >3m of clayey *terra rossa* sediment. B) The presence of a
679 debris cone similar to those described in the Naracoorte cave system (Moriarty et al.
680 2000) provides a plausible working model to explain the interlayering of different
681 sediment types (Fig 2E), the presence of abundant reworked litho-relicts (Fig. 3B,E), and
682 the high abundance of unassociated and disarticulated but well-preserved large-vertebrate
683 fossils. C) The PCS has evidence for pedogenesis and deep scouring of portions of the
684 *red facies* sediment, which likely occurred when the environment opened to the land
685 surface, thus allowing sediment and water from the surface to enter into the site. D) At
686 some point after the initiation of pedogenesis, the PCS flooded and a stagnant pond
687 developed accumulating at least 1.9 m of *dark facies* sediment that is rich in fossils and
688 pollen. E) Prior to discovery the PCS was buried beneath a thick blanket of Pleistocene
689 glacial till.

690 Historically the PCS region was characterized by broad leaf forest (E), but it
691 appears that during the Late Neogene the greater landscape was characterized by more
692 open conditions, but with abundant pine trees associated with the pond itself. The
693 formation of *terra rossa* suggest that temperatures were elevated and soils were freely
694 drained during the late Neogene.

Figure 1
[Click here to download high resolution image](#)

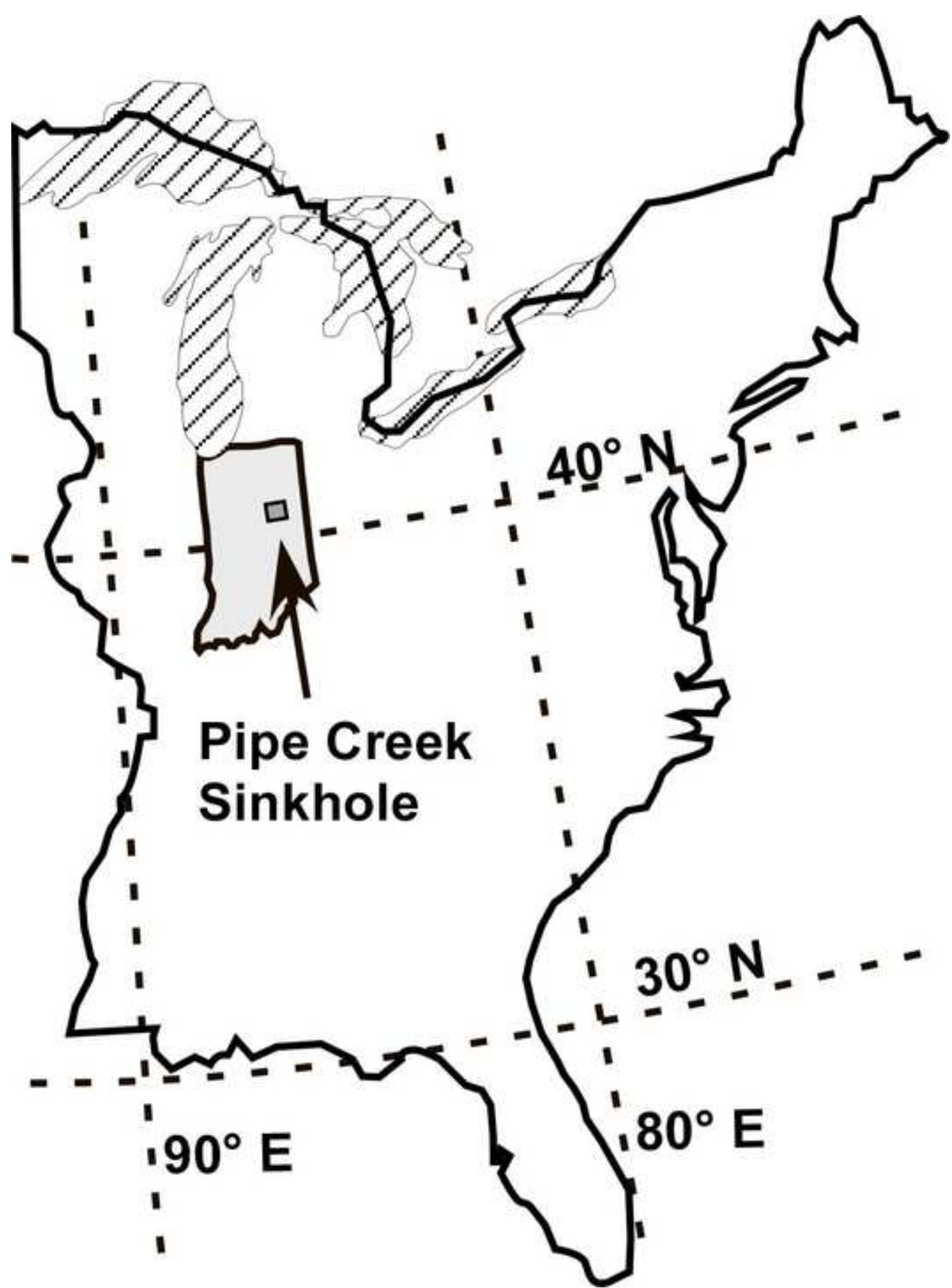


Figure 2
[Click here to download high resolution image](#)

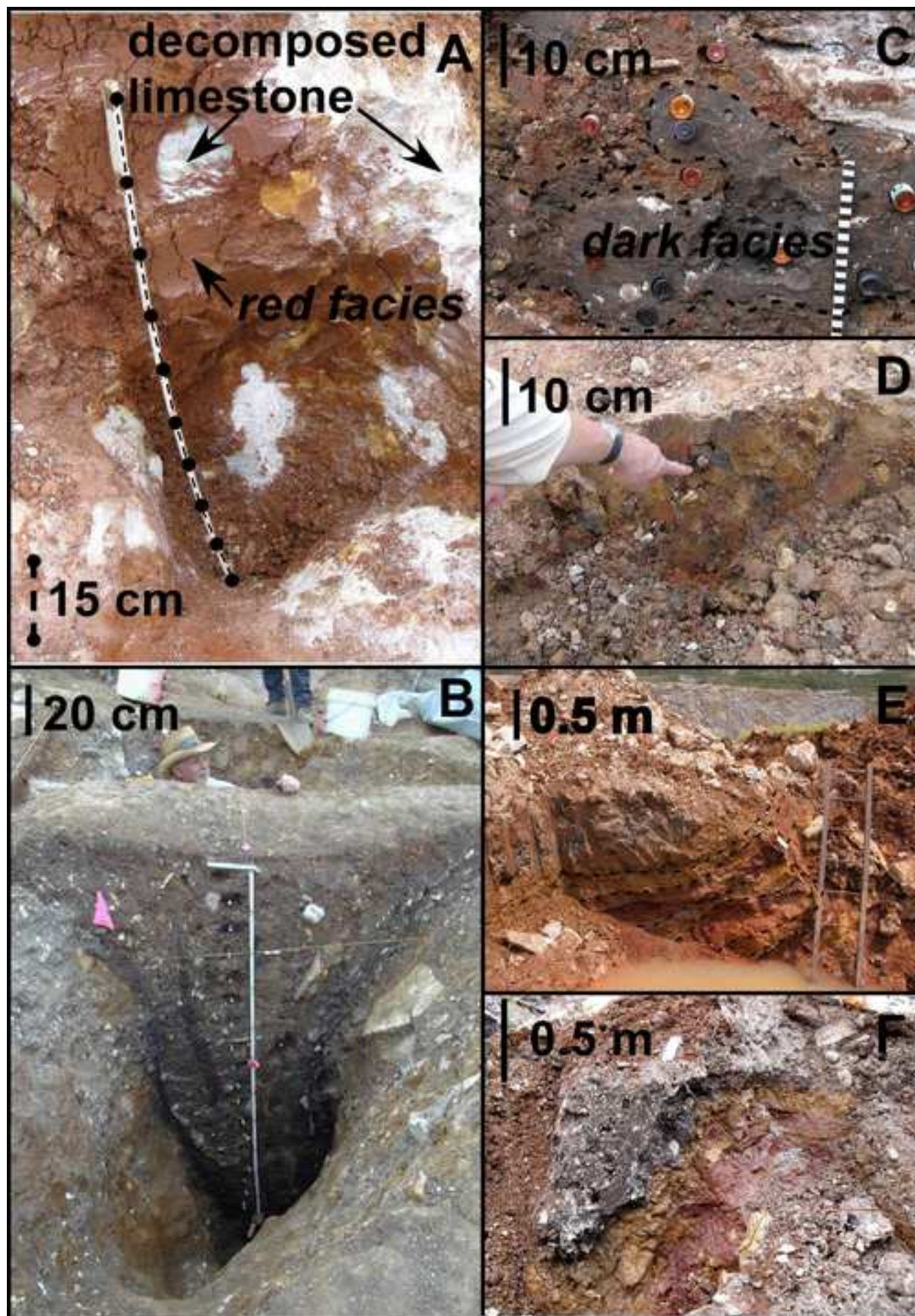


Figure 3
[Click here to download high resolution image](#)

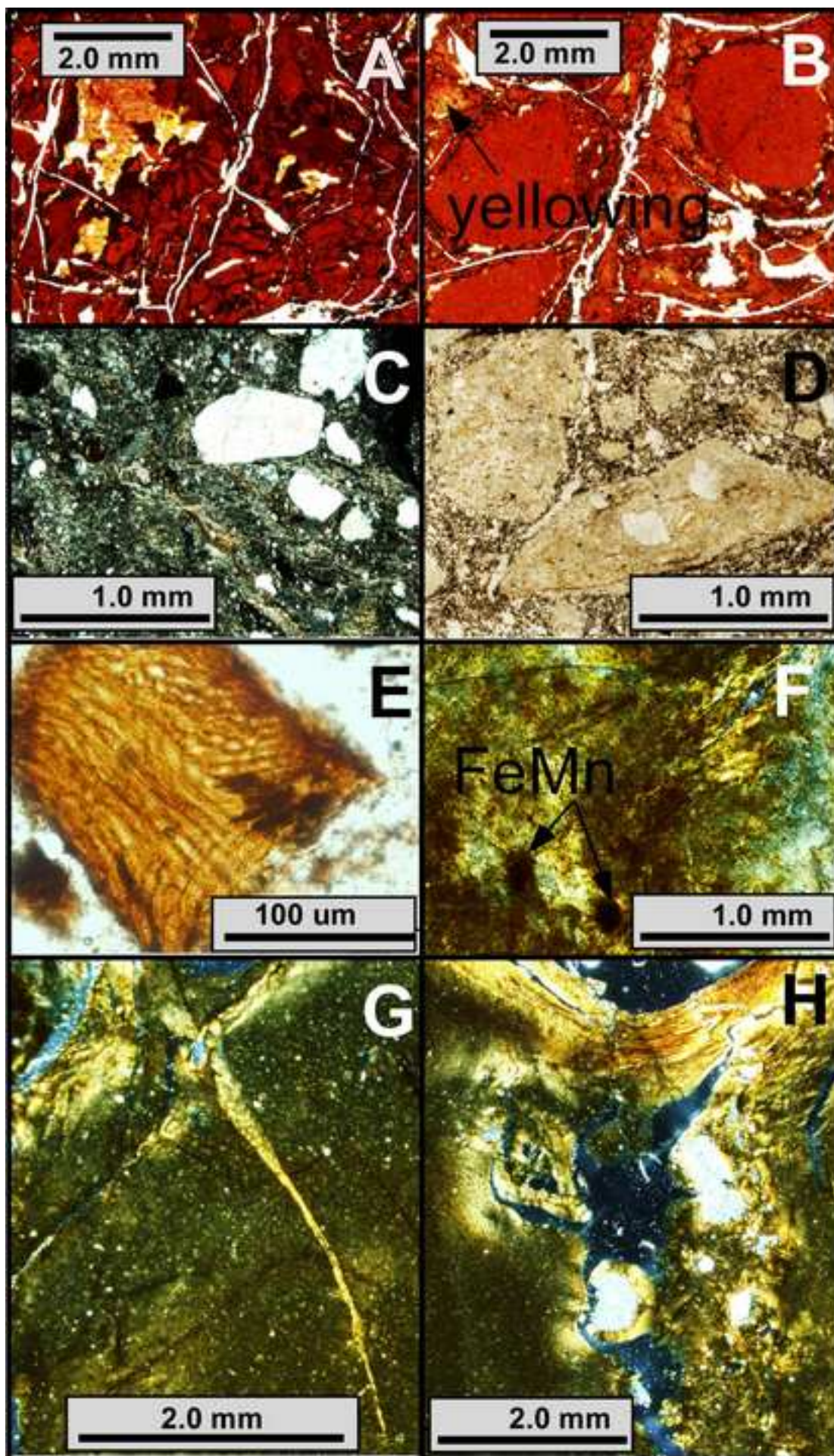


Figure 4
[Click here to download high resolution image](#)

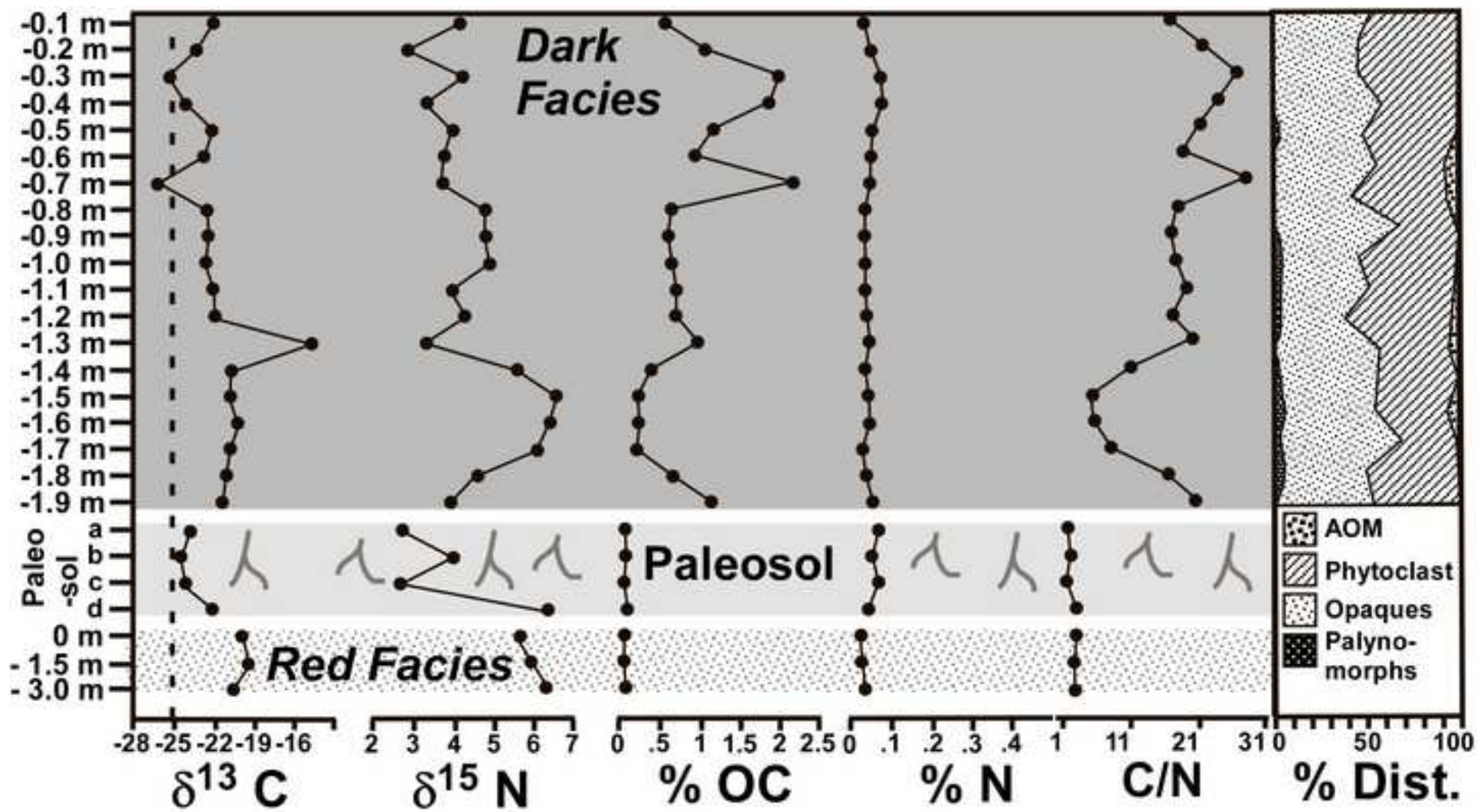


Figure 5
[Click here to download high resolution image](#)

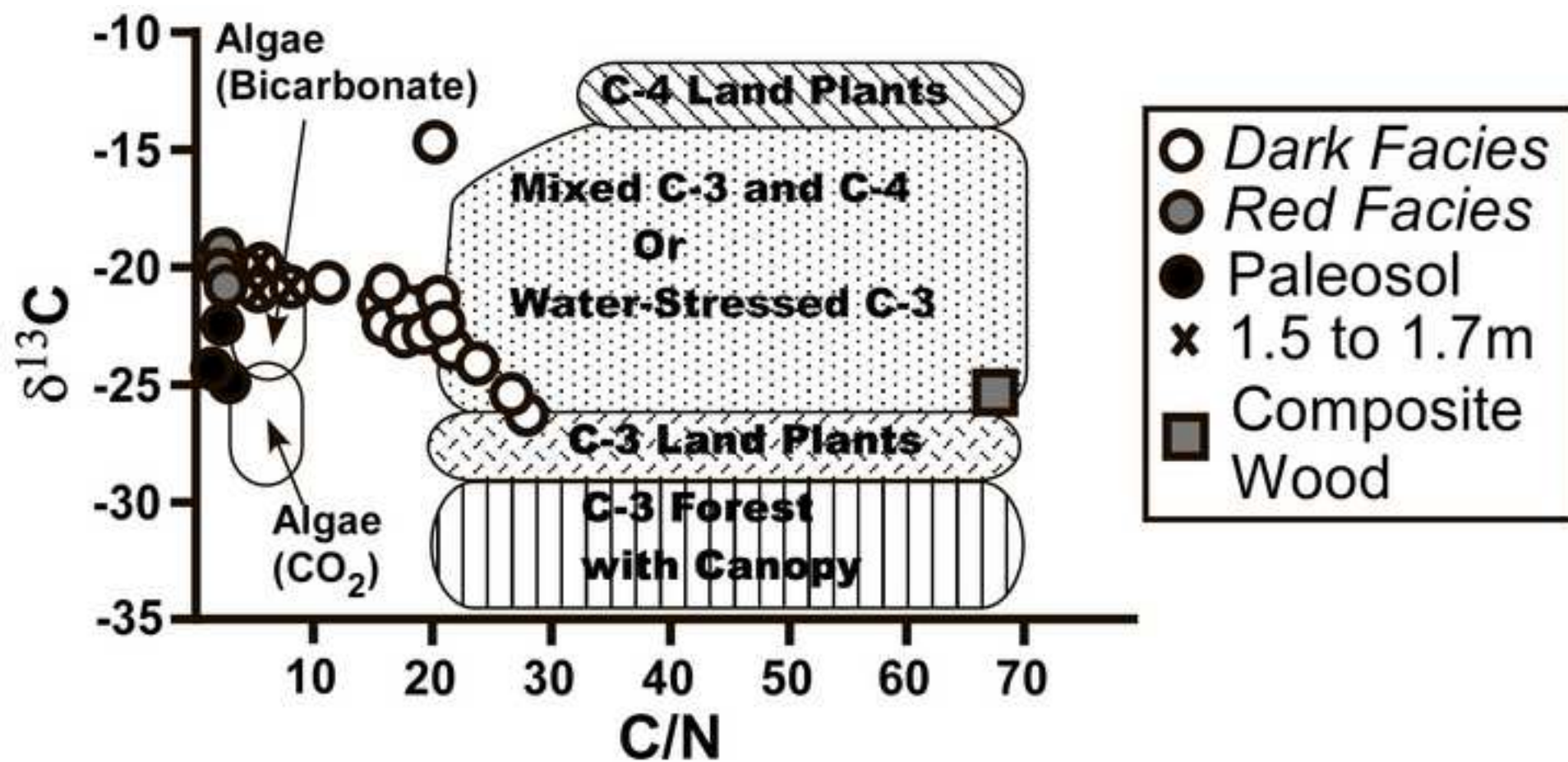


Figure 6

[Click here to download high resolution image](#)

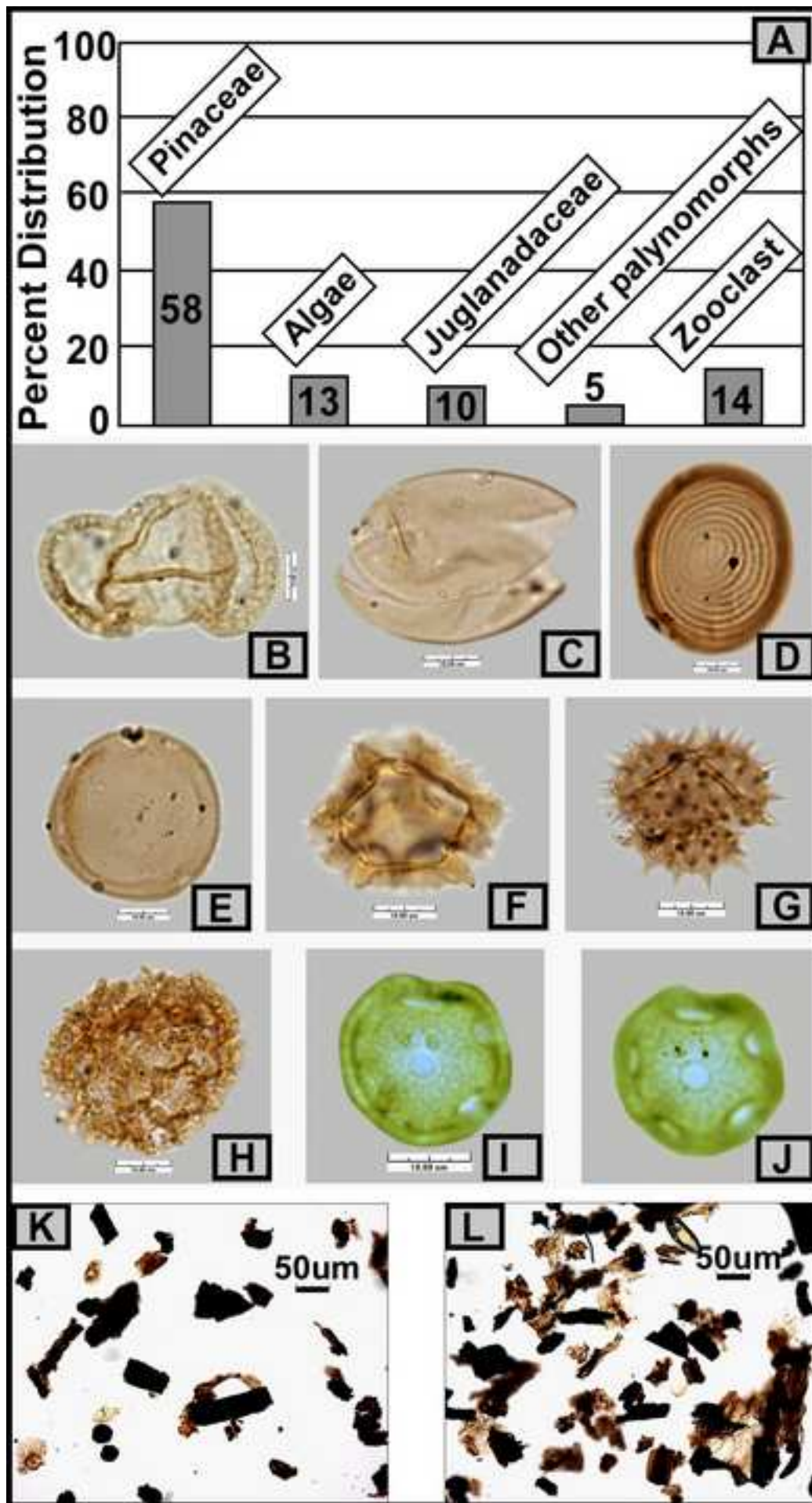


Figure 7
[Click here to download high resolution image](#)

